Ciencias Marinas Journal/Revista

Effect of a bacterial consortium on the growth, morphology, pigments, and toxicity of the dinoflagellate *Gymnodinium catenatum*

Dulce V Ramírez-Rodríguez[1], Christine J Band-Schmidt[1]*, Bárbara González-Acosta[1], Francisco E Hernández-Sandoval[2], Aldo Aquino-Cruz[3], Sonia I Quijano-Scheggia[4], José J Bustillos-Guzmán[2]

ARTICLE INFO

Article history:
Received 27 April 2023
Accepted 03 September 2023
Published 21 February 2024

LEER EN ESPAÑOL:
https://doi.org/10.7773/cm.y2024.3415

CORRESPONDING AUTHOR
* E-mail: cbands@ipn.mx

[1] Instituto Politécnico Nacional-Centro Interdisciplinario de Ciencias Marinas, 23096 La Paz, Baja California Sur, Mexico.
[2] Centro de Investigaciones Biológicas del Noroeste, 23096 La Paz, Baja California Sur, Mexico.
[3] Universidad Autónoma Metropolitana, Unidad Xochimilco, 04960 Mexico City, Mexico.
[4] Centro Universitario de Investigaciones Oceanológicas. Universidad de Colima, 28860 Manzanillo, Colima, Mexico.

ABSTRACT. *Gymnodinium catenatum*, a dinoflagellate that produces paralytic toxins, is one of the most studied dinoflagellate species. However, scarce information exists about its interaction with bacteria. In this study, the effect of a bacterial consortium in strains of *G. catenatum* was determined. Four strains of *G. catenatum* isolated from Bahía de Santiago, Colima; Lázaro Cárdenas, Michoacán; and Bahía Concepción and Bahía de La Paz, Baja California Sur were used. From the strain isolated from the coasts of Colima, a bacterial consortium was isolated with agar plates with GSe media that were incubated at a salinity of 34, at 24 °C in a L:D cycle of 12:12 h. *Gymnodinum catenatum* was cultivated in GSe media under the same conditions as the bacterial consortium. The interaction between these microorganisms was evaluated inoculating *G. catenatum* strains with the bacterial consortium. The maximum abundance, growth rate, chain length, toxin, and pigment profile were determined in *G. catenatum* with and without the bacterial consortium. In the presence of bacteria there was no clear effect on the growth, toxin profile, and toxin content in *G. catenatum*, but a significant increase in the chain length was observed. Changes in cell morphology were also observed. In addition, in the presence of the bacterial consortium, there was an increase in accessory pigments in most strains. Results suggest that the bacterial consortium could be a stress factor for *G. catenatum* and provide new perspectives on the interaction between bacteria and *G. catenatum.*

Key words: bacterial consortium, growth, dinoflagellate, pigments, paralytic toxins.

INTRODUCTION

Phytoplankton growth is controlled by a combination of hydrographic and physicochemical conditions such as temperature, light, and nutrients (Noman et al. 2019, Vives et al. 2022). However, biotic factors also have a synergistic effect on phytoplankton growth due to interactions with other microorganisms that favor the development of ecological relationships such as mutualism, allelopathy, predation, and/or grazing (Rooney-Varga et al. 2005).

In particular, dinoflagellates maintain associations with symbiotic bacteria that colonize the phycosphere. These proliferate with the compounds released by the algae and carry out a variety of biological functions that include the provision of essential vitamins, the production of growth-promoting compounds, and photosynthesis (Paul and Ponhert 2011, Jauzein et al. 2015); in addition, symbiotic bacteria can eliminate phytoplankton through the production of algaecides (Zheng et al. 2023). Bacteria also influence metabolism through microbial loop processes, which replenish and modulate the concentration of nutrient inputs (Azam 1998) and dissolved organic matter (Moran and Miller 2007). Despite the impact of the bacterial community on phytoplankton dynamics and biogeochemical cycles, the biological associations between bacteria and algae are still not fully understood (Jauzein et al. 2015). Algae–bacteria interactions are complex, in part because they can be species-specific and vary with environmental conditions (Mayali and Azam 2004, Grossart and Simon 2007). The bacteria–dinoflagellate relationship has been considered a mutualistic relationship because dinoflagellates are not the

Open Access
Online ISSN: 2395-9053
Screened via Similarity Check powered by iThenticate
https://doi.org/10.7773/cm.y2024.3415

only ones that obtain benefits from associating with bacterial communities; they, in turn, provide optimal habitat for the growth of bacteria through the production of organic compounds and a greater fixation surface (Seibold et al. 2001, Wang et al. 2014, Jauzein et al. 2015).

Gymnodinium catenatum is the only naked marine dinoflagellate that produces paralyzing toxins (Hallegraeff 1993) and is one of the most studied dinoflagellates in Mexico (Band-Schmidt et al. 2010). Research has focused on the dynamics of their proliferations (Hernández-Sandoval et al. 2009, Cortés-Altamirano et al. 2019), toxins (Band-Schmidt et al. 2006, Durán-Riveroll et al. 2017), autoecology (Band-Schmidt et al. 2004, 2014; Bustillos-Guzmán et al. 2012; Hernández-Sandoval et al. 2022), and trophic interactions (Palomares-García et al. 2006, Bustillos-Guzmán et al. 2013, Fernández-Herrera et al. 2016). Its presence has been reported in more than 23 countries (Hallegraeff et al. 2011) and has been associated with organism mortality and human poisonings (MacKenzie 2014, Chen 2018). In Mexico, in recent decades, reports of this species and its negative impacts have increased (Alonso-Rodríguez and Páez-Osuna 2003, Medina-Elizalde et al. 2018). Due to this, there is greater interest in describing the effects of the factors that regulate the growth and toxicity of this species (Hallegraeff et al. 2011).

Despite being a highly studied species, little is known about the interaction that exists between *G. catenatum* and the bacterial community. Some reports have shown that bacteria are essential for their growth and influence their toxicity, nutrient absorption, abundance, and growth rate, and can form mutualism relationships through mechanisms that are still unknown (Amin et al. 2007, Green et al. 2010, Bolch et al. 2011). Contrary responses have also been observed in the growth of *G. catenatum* depending on the genera of bacteria with which it interacts. Bacteria of the *Roseobacter* genus promote the cell death of *G. catenatum*; *Marinobacter* sp. and *Alcanivorax* sp. stimulate its growth (Bolch et al. 2017). The purpose of this study was to determine if, in the presence of a bacterial consortium isolated from a strain of *G. catenatum* from the coasts of Colima, strains of *G. catenatum* from other coastal regions of the Mexican Pacific would increase their growth rate and abundance and evaluate how the length of its chains, its morphology, the profiles of pigments and paralyzing toxins would be modified.

Materials and methods

Gymnodinium catenatum strains and cultivation conditions

Four non-axenic strains of *G. catenatum* isolated from vegetative cells during algal bloom events from various regions of the Mexican Pacific were used with the codes GCCV-7, GCMV-7, 62L, and G7 (Table 1). The strains were kept in GSe medium (Blackburn et al. 2001) with vermicomposting extract (Bustillos-Guzmán et al. 2015). In all experimental conditions, the cultures were kept at 24 ± 1 °C, with an illumination of 150 µmol photons·m^{-2}·s^{-1} using daylight fluorescent lamps with a photoperiod of 12h:12h L:D at a salinity of 34.

Obtainment and counts of the bacterial consortium

Bacterial cells were separated from the dinoflagellate of *G. catenatum* G7 strain by phototacticism. At 12 h, a 100-µL aliquot of the bacteria that migrated to the illuminated area was taken and seeded in GSe medium with 1.5% agar in Petri dishes in triplicate. A bacterial consortium composed of 3 colonies of bacteria with different morphologies was obtained using the cross-streaking method. The colonies were kept in the liquid GSe medium and agar under the mentioned conditions. Morphological identification was performed in an optical microscope using Gram staining. To determine if the bacteria were nitrogen fixers, they were grown in ASN-III medium without a nitrogen source (Rippka et al. 1891).

To quantify bacteria, 1-mL aliquots were collected and samples were diluted in a 1:2 proportion with 1% PBS, fixed with 4% formalin, and stored at 4 °C in the dark. After 24 h, a 1:15 dilution was carried out with 1% Tris-EDTA previously filtered through 0.22-µm polycarbonate membranes. Staining of bacteria was done following the method of Kepner and Pratt (1994) with the fluorochrome SYBR Gold to stain DNA. Observations were made in an epifluorescence microscope (Olympus CH30) under blue light emission, with a wavelength between 450 and 490 nm at 1,000×, in darkness. Counts were performed on an epifluorescence microscope

Table 1. *Gymnodinium catenatum* strains isolated from vegetative cells during algal blooms in various regions of the Mexican Pacific.

Code	Place and year of isolation	Isolated by
GCCV-7	Bahía de Concepción, B.C.S. 2000	C. Band-Schmidt
GCMV-7	Bahía de Mazatlán, Sin. 2013	L. Morquecho-Escamilla
G7	Bahía de Manzanillo, Col. 2010	S. Quijano-Scheggia
62L	Lázaro Cárdenas, Mich. 2005	M. Rodríguez-Palacio

(Olympus CH30) with a square ocular micrometer (10 × 10 mm), divided into 100 units. We considered 10 fields or those needed to complete a total of 300 cells (Kirchman et al. 1982, Sherr et al. 1993). The number of bacteria was determined with the following equation, with the corresponding settings for epifluorescence microscopy:

$$\text{cell} \cdot \text{mL}^{-1} = \frac{(N \times F \times d)}{V} \quad , \qquad (1)$$

where N is the average number of cells per reticle, F is the number of times the area of the reticle fits into the effective filtration area of the filter, d is the dilution, and V the filtered volume of the sample (mL); the filtration area was obtained from $\pi \cdot r^2$ (20,106 mm^2), and the reticle area was 0.01 mm^2 at 100×.

Curves, growth rates, and chain lengths of *Gymnodinium catenatum* in the presence and absence of the bacterial consortium

A total of 150 mL of GSe medium was placed in 250-mL Erlenmeyer flasks, and each *G. catenatum* strain was inoculated separately with an initial density of 500 cell·mL^{-1}, with and without adding the bacterial consortium, in triplicate. The microbial consortium was composed of 9,500 cell·mL^{-1} of filamentous bacteria, 70,000 cell·mL^{-1} of bacillus-type bacteria, and 9,000 cell·mL^{-1} of coccus-type bacteria. We took 2 mL of culture every second day until reaching the decay phase (maximum 26 days), fixing the samples with 1% Lugol (Throndsen 1979). Dinoflagellate counts were performed using a Sedgewick-Rafter chamber under an optical microscope (Labomed CXRII). The number and length of cell chains were recorded. In all treatments, morphological changes in live *G. catenatum* cells were recorded under a Zeiss Axioscope optical microscope with a ScopePhoto camera (version 3.0). The growth rate (K) was determined during the exponential growth phase, using the Guillard (1973) equation:

$$K = \frac{(\ln C2 - \ln C1)}{(t2 - t1)} \quad , \qquad (2)$$

where $C1$ is the number of cells per milliliter at time one ($t1$) and $C2$ is the number of cells per milliliter at time two ($t2$).

Pigments and paralyzing toxins

The pigment and toxin profiles of *G. catenatum* were determined in the presence and absence of the bacterial consortium during the exponential growth phase. For both analyses, 25-mL aliquots were filtered through 25-mm GF/F glass fiber membranes (Whatman, Springfield Mill, UK), and the samples were stored at –20 °C until analysis. Pigment analyses were performed by high-performance liquid chromatography (HPLC) on Agilent Technologies mod 1100 equipment (Santa Clara, USA) following the protocol of Vidussi et al. (1996). To identify and count pigments, the retention times and the light adsorption spectrum obtained with commercial standards (International Agency for Carbon 14 Determinations, Denmark) were used (Vidussi et al. 1996, Montoura and Repeta 1997).

To analyze toxins, extraction and hydrolysis were carried out according to the methods of Hernández-Sandoval et al. (2022). Toxin analyses were performed by HPLC on an Agilent Technologies mod 1260 Infinity II (Santa Clara, USA) according to the methods of Hummert et al. (1997) and Yu et al. (1998). Toxins were detected using a fluorescence detector (1260 FLD) with wavelengths at Ex 330 nm and Em 395 nm. To identify saxitoxin analogues, retention times were compared with commercial standard samples (NRC, Canada).

Statistical analyses

Differences in the maximum abundance of *G. catenatum* strains were determined with a univariate analysis of variance, the normality of the data was tested with the Kolmogorov–Smirnof test, and homoscedasticity with the Levene test. For data that did not conform to normality, a Kruskal–Wallis test was performed (Zar 1999). Differences in the length of cell chains and in the profile of paralyzing toxins were evaluated with the χ^2 statistical test, whereas differences in the profile of pigments and toxins were evaluated with the Student's t test (Zar 1999). When there were significant differences, post-hoc Tukey mean comparison tests (Day and Quinn 1989) were performed for homogeneous groups. Analyses were performed using Statistica v. 7.0 software (StatSoft, Inc.) with a significance level of 0.05.

Results

Bacterial consortium

We isolated a bacterial consortium associated with *G. catenatum* using the phototaxis and vertical migration technique. We obtained 3 populations of bacteria by cross-streak plating. The first population consisted of heterotrophic Gram-negative filamentous bacteria with a size of 7–10 µm; the second consisted of heterotrophic Gram-negative bacillus-type bacteria with a size of 5.00 ± 0.55 µm; the third consisted of Gram-negative, autotrophic, nitrogen-fixing, coccus-type bacteria with a size of 4.00 ± 0.86 µm. The bacterial consortium was composed of 9,500 cell·mL^{-1} of a filamentous bacteria, 70,000 cell·mL^{-1} of bacillus-type bacteria, and 9,000 cell·mL^{-1} of coccus-type bacteria.

Curves, growth rates, and chain lengths of *Gymnodinium catenatum* in the presence and absence of the bacterial consortium

Without the addition of the bacterial consortium, all *G. catenatum* strains showed a short acclimatization phase (if present), followed by an exponential phase and a pronounced

decay phase. The exponential phase in all strains started on day 2 and ended between days 14 and 20 (Fig. 1 a–d).

The growth of *G. catenatum* varied with each strain when inoculated with the bacterial consortium. In the presence of the bacterial consortium, the GCCV-7 strain prolonged the exponential phase to 22 d with respect to the control, which ended on day 12 (Fig. 1a). Maximum abundance with the inoculation of the bacterial consortium was significantly higher ($P < 0.05$) with respect to that of the control, namely 6,932 ± 26 and 6,463 ± 25 cell·mL^{-1}, respectively (Fig. 1a). In the presence of the consortium, the exponential phase in the GCMV-7 strain lasted 14 d, whereas in the control, it was prolonged to 20 d (Fig. 1b); in the presence of the consortium, maximum abundance was significantly higher ($P < 0.05$) (6,334 ± 25 cell·mL^{-1}) than in the control (2,840 ± 38 cell·mL^{-1}).

In strains G7 and 62L, the addition of the bacterial consortium did not favor the growth of the dinoflagellate. In strain G7, the exponential phase ended at 14 d with the inoculation of the consortium and at 16 d without it (Fig. 1c). In the presence of the bacterial consortium, the maximum abundance was 1,146 ± 5 cell·mL^{-1}, which was significantly lower ($P < 0.05$) than the maximum abundance without the bacterial consortium (1,625 ± 5 cell·mL^{-1}). In strain 62L, the exponential phase lasted until day 16 without the bacterial consortium and reached a maximum abundance of 6,444 ± 4 cell·mL^{-1}; with the bacterial consortium, the abundance was significantly lower ($P < 0.05$) 628 ± 317 cell·mL^{-1} (Fig. 1d).

The highest exponential growth rates without the bacterial consortium were obtained in strains GCCV-7 and 62L (0.215 ± 0.005 and 0.141 ± 0.002 d^{-1}, respectively), followed by strain G7 with a growth rate of 0.094 ± 0.017 d^{-1} and strain GCMV-7 with the lowest growth rate (0.079 ± 0.002 d^{-1}). With the addition of the bacterial consortium, strains GCCV-7, G7, and 62L significantly decreased ($P < 0.05$) their growth rates to 0.065 ± 0.00, 0.044 ± 0.017, and 0.0 d^{-1}, respectively; in strain GCMV-7, the growth rate increased significantly ($P < 0.05$) to 0.165 ± 0.001 d^{-1} (data not shown).

Without the addition of the bacterial consortium, the percentage of individual cells in the GCMV-7 strain increased until the sixth day of culture (from 22% to 50%). After this day, cells in chains composed mainly of 2–3 cells predominated and varied between 20% and 71% (Fig. 2a). With the bacterial consortium, the percentage of individual cells decreased significantly to less than 43% and chains of 4–6 cells represented between 20% and 43% ($P < 0.05$) (Fig. 2b).

Without the addition of the bacterial consortium, strain G7 had a higher percentage of single cells until day 8 and 10 (35%) (Fig. 2c). This strain had a predominance of chains of more than 4 cells (from 36% to 67%). In the presence of the bacterial consortium, single cells significantly increased (from 24% to 70%) ($P < 0.05$), followed by chains of 4 to 6 cells (from 19% to 44%) ($P < 0.05$) (Fig. 2d).

Without adding the bacterial consortium, in the GCCV-7 strain, individual cells increased from 19% to 70% until days 8–10 (Fig. 2e), followed by an increase in chain length. In the presence of the bacterial consortium, during most of the growth curve, the percentage of individual cells significantly decreased to between 3% and 32% ($P < 0.05$) and increased the formation of chains of 4–6 cells (between 30% to 62%) and of ≥7 cells (between 10% and 40%) (Fig. 2f).

In strain 62L, without the bacterial consortium, single cells predominated (between 18% and 54%) during most of the growth curve (Fig. 2g). In the presence of the bacterial consortium, the percentage of individual cells decreased significantly ($P < 0.05$) (between 5% and 12%), as did chains of 2–3 cells (between 15% and 26%) ($P < 0.05$); chains of 4–6 and ≥7 cells increased significantly ($P < 0.05$) (from 67% to 87%).

Morphological changes of *Gymnodinium catenatum* in the presence of the bacterial consortium

The morphological changes in *G. catenatum* with the addition of the bacterial consortium were the displacement in the sulcus and cingulum, the rupture of the cell membrane, the presence of trapezoidal cells, the displacement in cytoplasmic material, the presence of condensed chromosomes, and the presence of temporary cysts and lysis (Fig. 3). A high percentage of cells (80–90%) showed these changes 3 h after inoculating the bacterial consortium. Only strain G7, the strain from which the bacterial consortium was obtained, showed no changes in its morphology.

Temporary cysts (15%) were observed in the GCCV-7 strain during the decay phase. A high percentage of temporary cysts (95%) also inhibited the growth of strain 62L when the bacterial consortium was added. In the GCCV-7 and GCMV-7 strains, in addition to the morphological changes described above, when the bacterial consortium was added, the cultures showed a color change and acquired an intense green tone; this coloration occurred during the exponential phase; the growth of *G. catenatum* was not inhibited.

Profile of pigments and paralyzing toxins

The pigment profile in *G. catenatum* cultures in the presence and absence of the bacterial consortium consisted of 8 photosynthetic pigments. Chlorophyll *a* was the most abundant pigment (from 47.52 ± 2.52% to 52.96 ± 1.65%) with no significant differences between treatments; the percentage of chlorophyll *c*2, carotenoids (zeaxanthin, β-carotene), and xanthophylls (diadinoxanthin, dinoxanthin, diatoxanthin) varied between strains and some pigments varied between treatments. The presence of the bacterial consortium in strains GCMV-7 and GCCV-7 significantly increased ($P < 0.05$) the percentage of zeaxanthin (from 0.0 to 4.46 ± 0.57% and from 0.0 to 6.93 ± 3.81%, respectively) and β-carotene (from 0.24 ± 0.08 to 2.46 ± 0.58% and from 0.40 ± 0.06 to 2.83 ± 0.74%, respectively) ($P < 0.05$) (Fig. 4a, b). In the presence of the bacterial consortium, strain 62L showed no significant changes in pigment content ($P > 0.05$) (Fig. 4c); in strain G7,

the percentage of chlorophyll *c*2 and peridinin significantly increased ($P > 0.05$) and zeaxanthin and ß-carotene significantly decreased (Fig. 4d).

In all *G. catenatum* strains, 8 paralyzing toxin analogues were identified: C1/2, dcNEO, dcSTX, dcGTX 2/3, and GTX2/3. These were grouped based on the substituent group on the lateral chain into carbamoyl (GTX2/3), decarbamoyl (dcNEO, dcSTX, and dcGTX2/3), and N-sulfocarbamoyl (C1/2) toxins (Table 2). With the addition of the bacterial consortium, the GCMV-7 strain did not show significant changes in the toxin profile; N-sulfocarbamoyl toxins were the most abundant (between 23.40 ± 3.81 and 21.94 ± 3.78 pgSTX eq·cell^{-1}), followed by decarbamoyl (between 12.16 ± 0.52 and 15.35 ± 0.73 pgSTX eq·cell^{-1}) and carbamoyl (<1.24 pgSTX eq·cell^{-1}) (Table 2). In the GCCV-7 strain, the bacterial consortium significantly increased ($P < 0.05$) the content of the toxins N-sulfocarbamoyl (from 43.25 ± 6.99 to 84.03 ± 14.07 pgSTX eq·cell^{-1}), decarbamoyl (from 10.53 ± 0.43 to 14.77 ± 0.71 pgSTX eq·cell^{-1}), and carbamoyl (from 1.87 ± 0.10 to 4.41 ± 0.13 pgSTX eq·cell^{-1}). In the presence of the bacterial consortium, strain 62L showed lower ($P < 0.05$) contents of decarbamoyl toxins (from 84.23 ± 3.81 to 20.71 ± 0.92 pgSTX eq·cell^{-1}). In strain G7, the presence of the bacterial consortium decreased decarbamoyl toxins from 2.04 ± 0.16 to 0.69 ± 0.05 pgSTX eq·cell^{-1} and carbamoyl toxins did not exceed 1.15 pgSTX eq·cell^{-1} (Table 2).

In the presence of the bacterial consortium, the toxin content decreased significantly in strains 62L and G7 (from 126.35 ± 41.66 to 58.47 ± 18.34 and from 3.20 ± 1.02 to 1.76 ± 0.54 pgSTX eq·cell^{-1}, respectively). In the presence of the bacterial consortium, the toxin content of the GCCV-7 strain increased ($P < 0.05$) (from 55.63 ± 21.83 to 103.22 ± 43.29 pgSTX eq·cell^{-1}); this strain had the highest toxin content (Table 2).

Discussion

The study of bacteria–microalgae interactions in *G. catenatum* has become relevant in the past decade, with several aspects being described, such as the autonomous production of toxins by bacteria and their intervention in (1) the synthesis of toxins, (2) the reproductive process, (3) the direct or indirect influence on the development of certain stages of the life cycle of dinoflagellates, and (4) growth (Bolch et al. 2011, 2017; Albinsson et al. 2014; Jauzein et al. 2015). However, due to the complexity of algae–bacteria interactions, these need to be understood in strains from various geographical areas and environmental conditions. In this study,

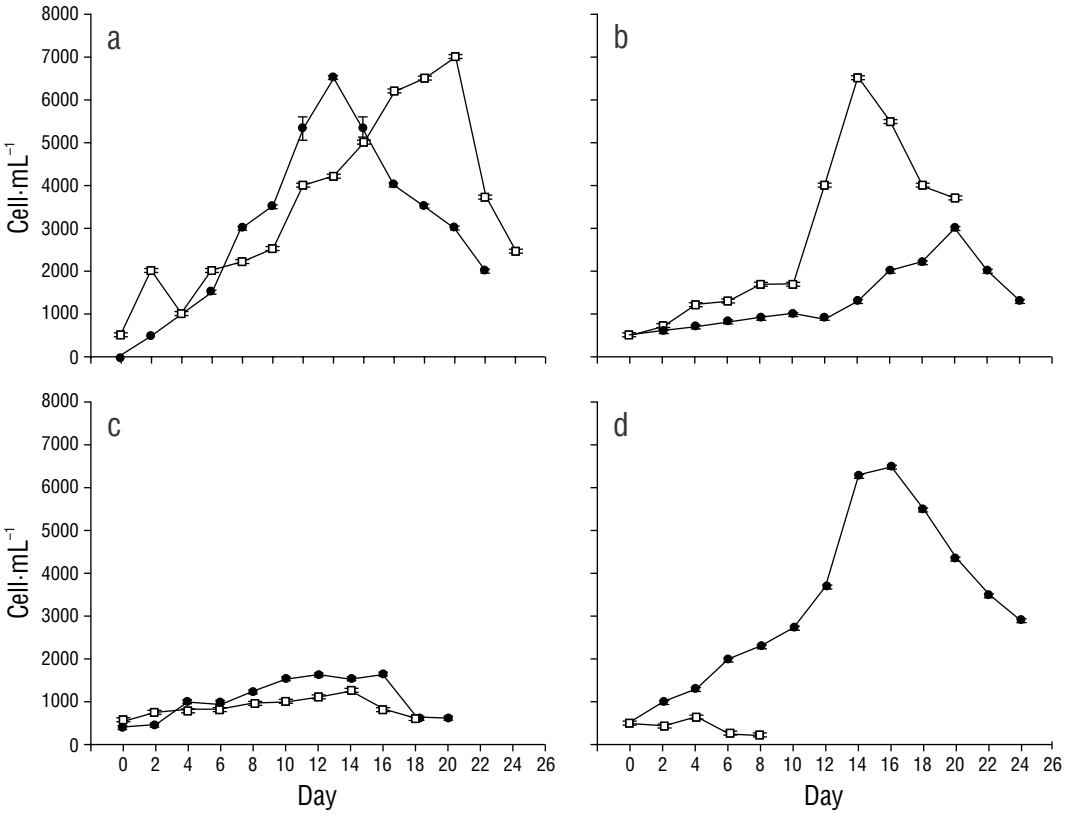

Figure 1. Growth curves of *Gymnodinium catenatum* in GSe medium at 24 °C, salinity of 34, and 12:12 h L:D cycle in the presence of the bacterial consortium (empty boxes) and without adding the bacterial consortium (black circles). Strains: (**a**) GCCV-7. (**b**) GCMV-7. (**c**) G7. (**d**) 62L. Vertical lines: ds.

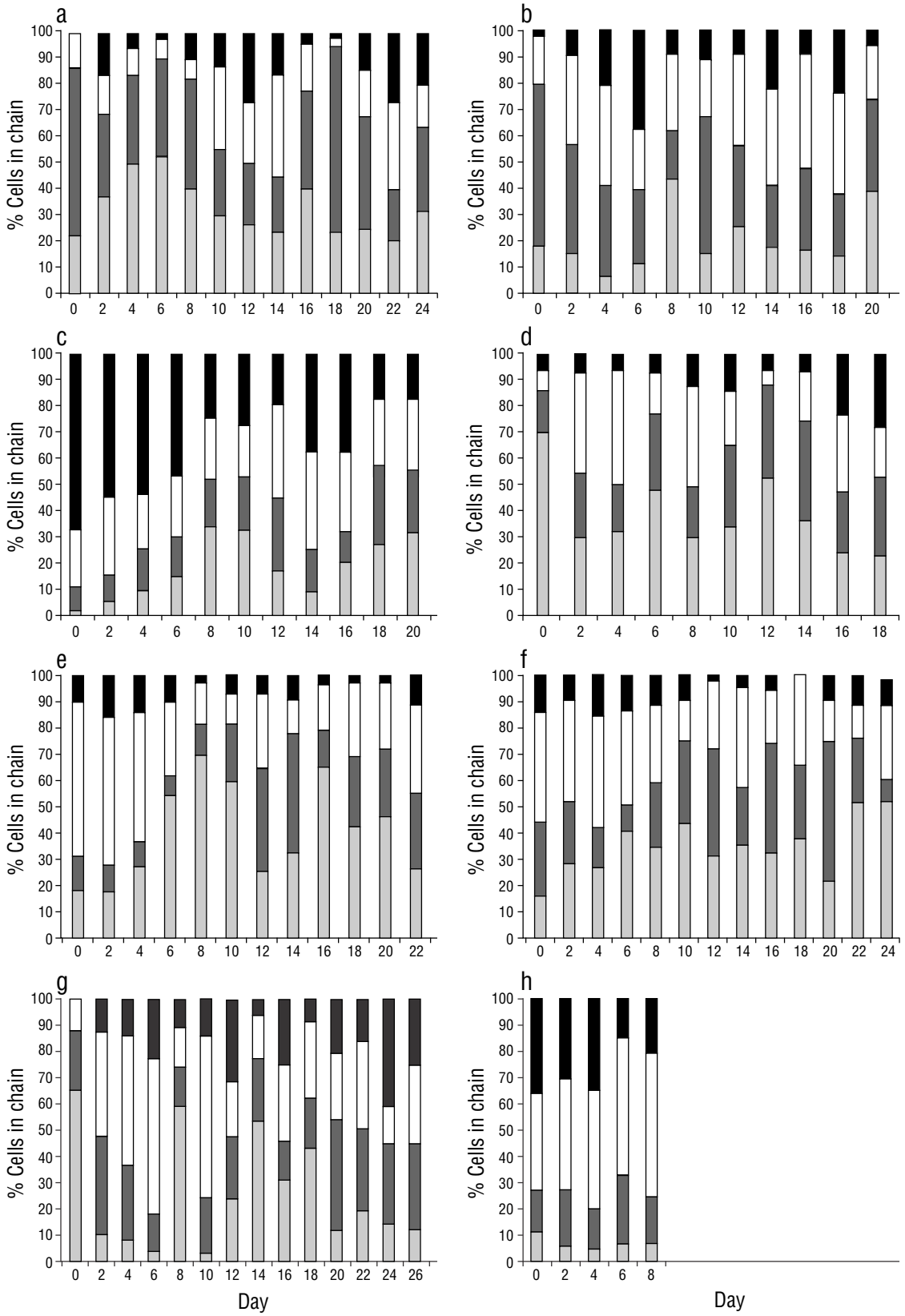

Figure 2. Cell chains during the growth curve of *Gymnodinium catenatum* in the presence and absence of the bacterial consortium (BC). Light gray: individual cells. Dark gray: chains of 2–3 cells. White: chains of 4–6 cells. Black: chains of ≥7 cells. (**a**) strain GCMV-7 without BC; (**b**) strain GCMV-7 with BC; (**c**) strain G7 without BC; (**d**) strain G7 with BC; (**e**) strain GCCV-7 without BC; (**f**) strain GCCV-7 with BC; (**g**) strain 62L without BC; (**h**) strain 62L with BC.

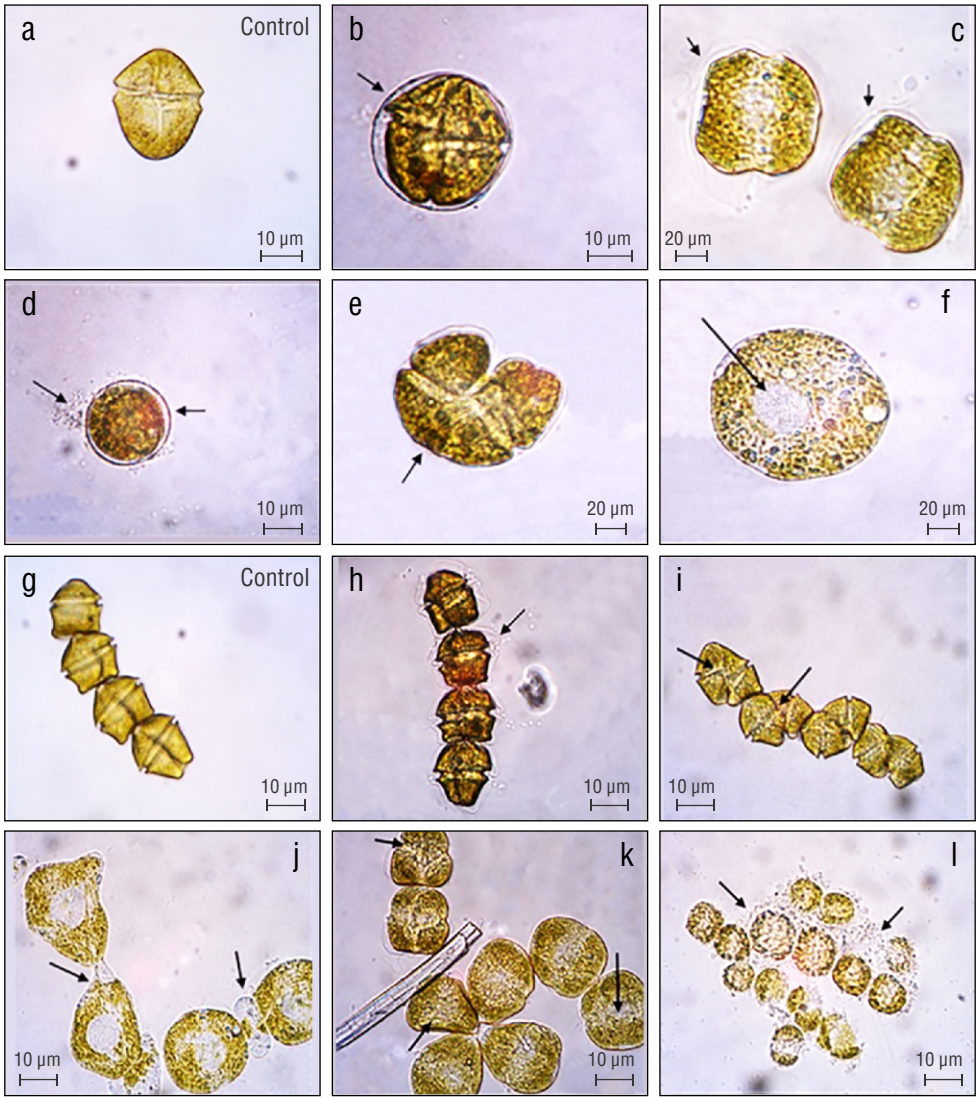

Figure 3. Morphology of *Gymnodinium catenatum* in the presence and absence of the bacterial consortium. (**a**) Single cell (control). (**b**) Cell surrounded by a membrane characteristic of a temporal cyst. (**c**) Membrane rupture, loss of flagellum, displacement of the cingulum and sulcus. (**d**) Temporal cyst and bacteria. (**e**) Trapezoidal cell. (**f**) Round cell with evident nucleus and condensed chromosomes. (**g**) Chain of cells (Control). (**h**) Chain cells surrounded by hyaline membrane. (**i**) Displacement of the cingulum and sulcus. (**j**) Membrane rupture. (**k**) Displacement in the cytoplasm. (**l**) Lysis.

the effect of a bacterial consortium on the growth, abundance, morphology, chain length, pigment profile, and paralyzing toxins in *G. catenatum* was evaluated in 4 strains from different regions of the Mexican Pacific.

It has been reported that 15 to 24 bacterial genotypes make up the bacterial community associated with *G. catenatum* strains (Green et al. 2004, 2010). However, even though the community is so variable, previous studies have concluded that the effect of the bacterial community on the dinoflagellate is caused by the dominance of 1 or 2 species, not by the coexistence of these, because the dominant bacteria affect the growth of the dinoflagellate and inhibit the growth of the rest of the associated bacteria in mixed cultures (Albinsson et al. 2014). The growth curves of *G. catenatum* showed 2 growth patterns (Fig. 1a–d) in the presence of the bacterial consortium. The first is greater growth of the dinoflagellate, reflected in greater abundance. When cultured with the bacterial consortium, the GCCV-7 strain, in addition to increasing in abundance, reached the exponential growth phase in a greater number of days and had a lower growth rate (Fig. 1a). This coincides with what was reported for strains of *Alexandrium* spp. where the presence of bacteria prolonged exponential growth, which modulated the availability of nutrients with lower growth rates, which derived from growth dormancy (Hold et al. 2001). The second pattern observed was growth inhibition in *G. catenatum* strains 62L and G7 (Fig. 1c, d). In strain 62L, a significant decrease in abundance of more than 90% was observed with the addition

of the bacterial consortium. Alavi et al. (2001) and Matsumoto (2011) described a similar response. Alavi et al. (2001) evaluated the effect of physical interaction on 4 strains of the dinoflagellate *Pfiesteria* sp. in the presence of a bacterial consortium made up of 34 species and obtained an inhibition in the growth of *Pfiesteria* sp., which grew again when the cells were re-isolated in the absence of the bacterial consortium. On the other hand, Matsumoto (2011) evaluated the effect of bacterial cell filtrates from *Alcanivorax* sp. in *G. catenatum* and found that they inhibited the growth of the dinoflagellate, contrary to what was observed in experiments with cell contact, where the growth of *G. catenatum* was greater. This behavior could be due to bacteria releasing algaecides into the culture medium; nevertheless, neither Alavi et al. (2001) nor Matsumoto (2011) evaluated this parameter, but their results suggest that the growth-promoting substance is not exuded into the culture medium but rather that the species require being in contact to promote their growth, in addition to the fact that the growth dynamics established depend on the species of bacteria, which encourages the formation of various ecological associations (Skovgaard 2000).

Chain length in *G. catenatum* is an indicator of stress conditions, such as culture age (Blackburn et al. 1989, Band-Schmidt et al. 2004); extreme salinity, light, and temperature (Band-Schmidt et al. 2014; Vale 2015, 2017); limiting concentrations of phosphates and nitrates (Lin et al. 2022); and allelopathy (Fernández-Herrera et al. 2016, 2021; Band-Schmidt et al. 2020). It has been proposed that alterations in length patterns in the natural environment can affect the vertical migration speed of this dinoflagellate (Fraga et al. 1989, Vale 2015). The increase in the percentage of chain cells in the presence of the bacterial consortium in this work could indicate that bacteria promote chain formation. The percentage of long chains in strain G7 did not increase (Fig. 2d); this could be because the bacterial consortium was isolated from this strain.

Several studies of bacteria–microalgae interactions have focused on the influence of bacteria on the germination of resting cysts in *G. catenatum*. Newly germinated cells of *G. catenatum* require the presence of bacteria from the *Marinobacter* sp. and *Brachybacterium* sp. genera to survive and grow (Bolch et al. 2011). In this study, temporary cysts of *G. catenatum* formed when in contact with the bacterial consortium. Morphological changes were also observed in *G. catenatum* suggesting that these alterations could influence its life cycle: loss of flagella; displacement in the cytoplasm, cingulum, and sulcus; and an evident nucleus with condensed chromosomes, characteristic of the fusion of gametes (Fig. 3), which was previously described by Figueroa et al. (2006, 2008). These observations support one of the hypotheses established by the same authors that indicates that sexual processes are triggered as a result of the addition of nutrients, perhaps coming from bacterial exudates.

When *G. catenatum* was exposed to cells from other phytoplankton species or their filtrates, changes in its morphology were also observed, such as a decrease in the length of cell chains, formation of temporary cysts, and lysis (Fernández-Herrera et al. 2016, 2021; Band-Schmidt et al. 2020), which demonstrated that direct contact between phytoplankton species can also modify the dinoflagellate population structure.

The pigment profile of *G. catenatum* is made up of 8 pigments: chlorophyll *a*, chlorophyll *c*2, peridinin, zeaxanthin, diadinoxanthin, dinoxanthin, diatoxanthin, and β-carotene, coinciding with the pigment profile reported by Hallegraeff

Table 2. Paralyzing toxin profile and toxin content of *Gymnodinium catenatum* strains in the presence and absence of the bacterial consortium in the late exponential phase.

	N-sulfocarbamoyl	Decarbamoyl	Carbamoyl	Toxin content
Code		pg STXeq·cell^{-1}		
GCMV-7	23.40 ± 3.81	15.35 ± 0.73	1.00 ± 0.08	39.74 ± 11.35
GCMV-7 + BC	21.94 ± 3.78	12.16 ± 0.52	1.24 ± 0.07	35.33 ± 10.36
GCCV-7	43.25 ± 6.99	10.53 ± 0.43	1.87 ± 0.10	55.63 ± 21.83
GCCV-7 + BC	84.03 ± 14.07	14.77 ± 0.71	4.41 ± 0.13	103.22 ± 43.29
62L	41.18 ± 6.87	84.24 ± 3.81	0.94 ± 0.08	126.35 ± 41.66
62L + BC	37.18 ± 6.65	20.71 ± 0.92	0.57 ± 0.08	58.47 ± 18.34
G7	0.01 ± 0.04	2.04 ± 0.16	1.15 ± 0.21	3.20 ± 1.02
G7 + BC	-	0.69 ± 0.05	1.06 ± 0.18	1.76 ± 0.54

+BC: with bacterial consortium

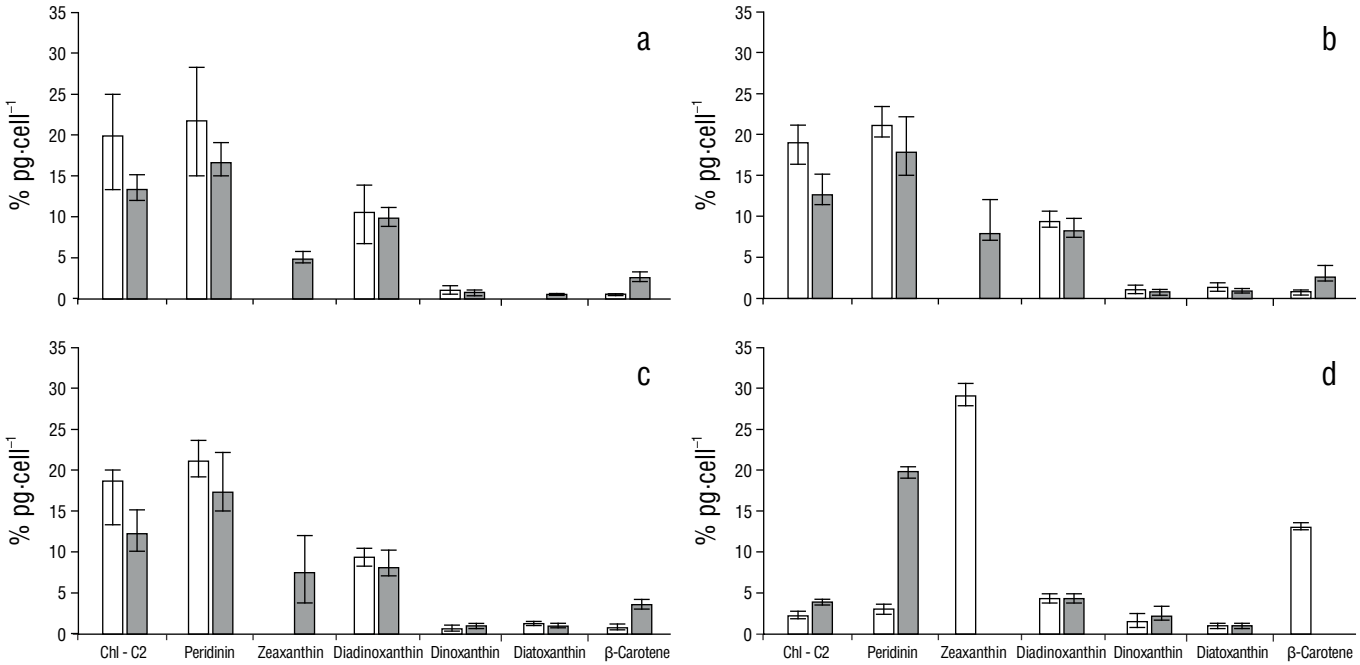

Figure 4. *Gymnodinium catenatum* pigments in the presence and absence of the bacterial consortium (BC). Strains: (**a**) GCMV-7; (**b**) GCCV-7; (**c**) G7; (**d**) 62L. White bars: without BC. Gray bars: with BC. Vertical lines: ds. Chlorophyll *a* is not included.

et al. (1991). Given that the only variant in the experiments was the addition of the bacterial consortium, it is assumed that pigment content varied with the presence/absence of the consortium; this last stress factor modified the photosynthetic capacity of the dinoflagellate because it modified the content of accessory pigments (Fig. 4).

The paralyzing toxin profile of *G. catenatum* includes at least 3 dozen analogues described in various strains and geographical populations, which are characterized by the dominance of sulfocarbamoyl toxins that represent more than 85 mol%, followed by decarbamoyl and, finally, carbamoyl with a percentage <1% (Negri et al. 2007, Band-Schmidt et al. 2019). Although it has been determined that the presence, absence, and proportion of analogues varies between strains, there is a high similarity in the profile of paralyzing toxins between ecotypes, suggesting low genetic variability between populations (Cembella and Band-Schmidt 2018). The toxin profile of the strains in this study agrees with previous reports (Band-Schmidt et al. 2010). Most strains, with the exception of strain G7, showed a dominance of sulfocarbamoyl toxins, and a relative abundance greater than 70 mol% was recorded. Strain G7 was characterized by the dominance of decarbamoyl toxins, followed by sulfocarbamoyl and carbamoyl toxins. This profile has also been reported in environmental samples of *G. catenatum* (Gárate-Lizárraga et al. 2006). Saxitoxin analogues from the carbamoyl group (GTX2/3) were found in low proportions, <2% of the total, which is characteristic of the species (Hallegraeff et al. 2011). In the GCCV-7 strain, the presence of the bacterial consortium increased the content of sulfocarbamoyl toxins and decreased the content of carbamoyl toxins; whereas in strains 62L and G7, the content of decarbamoyl analogues decreased (Table 2).

The toxin content of this species is relatively low compared to those of other species, and differences have been reported between environmental samples of natural *G. catenatum* and samples obtained from laboratory strains, in addition to differences in toxicity depending on the origin of the strain (Band-Schmidt et al. 2006, Negri et al. 2007). In this study, the strain from the coasts of Michoacán had the highest toxin content, followed by the strains from Bahía Concepción, Bahía de Mazatlán, and, finally, the strain from Manzanillo, which varied greatly from 1.76 ± 0.54 to 103.22 ± 43.29 pgSTX eq·cell^{-1}. Nonetheless, it is important to note that data from a single strain from each geographic region is insufficient to confirm these differences in toxin content between various geographic regions.

The addition of the bacterial consortium did not show a clear pattern in the toxin content of the strains. The toxin content increased in the GCCV-7 strain, whereas it decreased in the 62L and G7 strains and showed no significant changes in the GCMV-7 strain. Toxin content in *G. catenatum* strains isolated from Mexican coasts has shown variability, and records show values from 2 to 370 pgSTX eq·cell^{-1} (Band-Schmidt et al. 2005, 2006; Fernández-Herrera et al. 2022). No clear relationship has been found with temperature (Band-Schmidt et al. 2014) or N:P ratios (Bustillos-Guzmán et al. 2012, Hernández-Sandoval et al. 2022), which suggests that the differences are strain-specific. Only in the case of the exposure of *G. catenatum* to culture media of *Chattonella marina* and *Gymnodinium impudicum* was there an increase in the toxin

content (Fernández-Herrera et al. 2022), which suggests that this increase could be a survival strategy of *G. catenatum* in the presence of other phytoplankton species.

With the addition of the bacterial consortium, *G. catenatum* showed no clear effect on growth, abundance, toxin profile, and toxin content, but it did show an increase in the number of chain cells. In addition, changes in cellular morphology were observed. In the presence of the bacterial consortium, in most strains, the content of accessory pigments (zeaxanthin, diatoxanthin, and β-carotene) increased, which suggests that bacteria could be stress agents for *G. catenatum*, which provides new perspectives on the interaction between bacteria and dinoflagellates.

Acknowledgments

This research was funded by the institutional project SIP (20231019) and the SEP-CONACyT projects (178227 and A1-S-14968). We thank the Programa Interinstitucional para el Fortalecimiento de la Investigación y el Posgrado del Pacífico, CIBNOR with its PACE, CONACyT (grant 21751), and the Red Temática de Florecimientos Algales Nocivos for the financial support received. We thank the CIBNOR Marine Dinoflagellate Collection, MC Rodríguez Palacio from UAM for providing some of the strains used, and Adriana Landa Blanco from the CIBNOR Scientific Extension and Dissemination Department for editing the figures.

English translation by Claudia Michel-Villalobos.

References

Alavi M, Miller T, Erlandson K, Schneider R, Belas R. 2001. Bacterial community associated with *Pfiesteria*-like dinoflagellate cultures. Environ Microbiol. 3:380-396. https://doi.org/10.1046/j.1462-2920.2001.0

Albinsson ME, Negri AP, Blackburn SI, Bolch CJS. 2014. Bacterial community affects toxin production by *Gymnodinium catenatum*. PLoS ONE. 9:e104623. https://doi.org/10.1371/journal.pone.0104623

Alonso-Rodríguez R, Páez-Osuna F. 2003. Nutrients, phytoplankton and harmful algal blooms in shrimp ponds: a review with special reference to the situation in the Gulf of California. Aquaculture. 219:317-336. https://doi.org/10.1016/S0044-8486(02)00509-4

Amin S, Küpper FC, Green DH, Harris WR, Carrano CJ. 2007. Boron binding by a siderophore isolated from marine bacteria associated with the toxic dinoflagellate *Gymnodinium catenatum*. J Am Chem Soc. 129:478-479. https://doi.org/10.1021/ja067369u

Azam F. 1998. Microbial control of oceanic carbon flux: the plot thickens. Science. 280:694-696.

Band-Schmidt CJ, Bustillos-Guzmán J, Gárate-Lizárraga I, Lechuga-Devéze CH, Reinhardt K, Luckas B. 2005. Paralytic shellfish toxin profile in strains of the dinoflagellate *Gymnodinium catenatum* Graham and the scallop *Argopecten ventricosus* G.B. Sowerby II from Bahía Concepción, Gulf of California, Mexico. Harmful Algae. 4(1):21-31. https://doi.org/10.1016/j.hal.2003.10.004

Band-Schmidt CJ, Bustillos-Guzmán JJ, Hernández-Sandoval FE, Núñez-Vázquez EJ, López-Cortés DJ. 2014. Effect of temperature on growth and paralytic toxin profiles in isolates of *Gymnodinium catenatum* (Dinophyceae) of the Pacific coast of Mexico. Toxicon. 90:199-212. https://doi.org/10.1016/j.toxicon.2014.08.002

Band-Schmidt CJ, Bustillos-Guzmán JJ, López-Cortés DJ, Gárate-Lizárraga I, Núñez-Vázquez E, Hernández-Sandoval, FE. 2010. Ecological and physiological studies of *Gymnodinium catenatum* in the Mexican Pacific: a review. Mar Drugs. 8:1935-1961. https://doi.org/10.3390/md8061935

Band-Schmidt CJ, Bustillos-Guzmán JJ, Morquecho L, Gárate-Lizárraga I, Alonso-Rodríguez R, Reyes-Salinas A, Erler K, Luckas B. 2006. Variations of PSP toxin profiles during different growth phases in *Gymnodinium catenatum* (Dinophyceae) strains isolated from three locations in the Gulf of California, Mexico. J Phycol. 42:757-768. https://doi.org/10.1111/j.1529-8817.2006.00234.x

Band-Schmidt CJ, Durán-Riveroll LM, Bustillos-Guzmán JJ, López-Cortés DJ, Núñez-Vázquez EJ, Hernández-Sandoval FE, Ramírez-Rodríguez DV. 2019. Paralytic toxin producing dinoflagellates in Latin America: Ecology and Physiology (a review). Front Mar Sci. 6:42. https://doi.org/10.3389/fmars.2019.00042

Band-Schmidt CJ, Morquecho L, Lechuga-Devéze CH, Anderson DM. 2004. Effects of growth medium, temperature, salinity and seawater source on the growth of *Gymnodinium catenatum* (Dinophyceae) from Bahía Concepción, Gulf of California, Mexico. J Plankton Res. 26:1459-1470. https://doi.org/10.1093/plankt/fbh133

Band-Schmidt CJ, Zumaya-Higuera MG, López-Cortés DJ, Leyva-Valencia I, Quijano-Scheggia SI, Hernández-Guerrero CJ. 2020. Allelopathic effects of *Margalefidinium polykrikoides* and *Gymnodinium impudicum* in the growth of *Gymnodinium catenatum*. Harmful Algae. 96:101846. https://doi.org/10.1016/j.hal.2020.101846

Blackburn SI, Bolch CJS, Haskard KA, Hallegraeff GM. 2001. Reproductive compatibility among four global populations of the toxic dinoflagellate *Gymnodinium catenatum* (Dinophyceae). Phycol. 40:78-87. https://doi.org/10.2216/i0031-8884-40-1-78.1

Blackburn SI, Hallegraeff GM, Bolch CJ. 1989. Vegetative reproduction and sexual life cycle of the toxic dinoflagellate *Gymnodinium catenatum* from Tasmania, Australia. J Phycol. 25:577-590. https://doi.org/10.1111/j.1529-8817.1989.tb00264.x

Bolch CJS, Bejoy TA, Green DH. 2017. Bacterial associates modify growth dynamics of the dinoflagellate *Gymnodinium catenatum*. Front Microbiol. 8:670. https://doi.org/10.3389/fmicb.2017.00670

Bolch CJ, Subramanian TA, Green HG. 2011. The toxic dinoflagellate *Gymnodinium catenatum* (Dinophyceae) requires marine bacteria for growth. J Phycol. 47:1009-1022. https://doi.org/10.1111/j.1529-8817.2011.01043.x

Bustillos-Guzmán JJ, Band-Schmidt CJ, Durán-Riveroll LM, Hernández-Sandoval FE, López-Cortés, DJ, Núñez-Vázquez EJ, Cembella A, Krock B. 2015. Paralytic toxin profile of the marine dinoflagellate *Gymnodinium catenatum* Graham from the Mexican Pacific as revealed by LC-MS/MS. Food Addit Contam Part A. 32:1-15. https://doi.org/10.1080/19440049.2014.1000978

Bustillos-Guzmán JJ, Band-Schmidt CJ, López-Cortés DJ, Gárate-Lizárraga I, Núñez-Vázquez EJ, Hernández-Sandoval FE. 2012. Variaciones en el crecimiento y toxicidad en *Gymnodinium catenatum* Graham del Golfo de California bajo diferentes proporciones de nitrógeno y fósforo. Cienc Mar. 38:101-117.

Bustillos-Guzmán JJ, Band-Schmidt CJ, López-Cortés DJ, Hernández-Sandoval FE, Núñez-Vázquez E, Gárate-Lizárraga I. 2013. Pastoreo del dinoflagelado *Noctiluca scintillans* sobre el dinoflagelado productor de toxinas paralizantes *Gymnodinium catenatum*: ¿Elimina el pastoreo células durante un florecimiento? Cienc Mar. 39:291-302.

Cembella A, Band-Schmidt CJ. 2018. *Gymnodinium catenatum*. Harmful algal species fact sheets. In: Shumway SE, Burkholder JM, Morton SL (eds.), Harmful Algal Blooms: A compendium desk reference. Hoboken (USA): Wiley Blackwell. p. 605-611.

Chen H. 2018. Emergency treatment and reflection of red tide event of *Gymnodinium catenatum* in Fujian Sea area in 2017. J Fisheries Res. 40(4):308-314.

Cortés-Altamirano R, Alonso-Rodríguez R, Salas-de-León DA. 2019. Historical observations of algal blooms in Mazatlan Bay, Sinaloa, Mexico (1979-2014). PLoS ONE. 14(1):e0210631. https://doi.org/10.1371/journal.pone.0210631

Day RW, Quinn GP. 1989. Comparisons of treatments after an analysis of variance in ecology. Ecol Mon. 59(4):433-463. https://doi.org/10.2307/1943075

Durán-Riveroll L, Krock B, Cembella A, Peralta-Cruz J, Bustillos-Guzmán JJ, Band-Schmidt CJ. 2017. Characterization of benzoyl saxitoxin analogs from the toxigenic marine dinoflagellate *Gymnodinium catenatum* by hydrophilic interaction liquid ion chromatography-tandem mass spectrometry. Nat Prod Chem Res. 5:275.

Fernández-Herrera LJ, Band-Schmidt CJ, López-Cortés DJ, Hernández-Guerrero CJ, Bustillos-Guzmán JJ, Núñez-Vázquez E. 2016. Allelopathic effect of *Chattonella marina* var. *marina* (Raphidophyceae) on *Gymnodinium catenatum* (Dinophycea). Harmful Algae. 51:1-9. https://doi.org/10.1016/j.hal.2015.10.009

Fernández-Herrera LJ, Band-Schmidt, CJ, Zenteno-Savín T, Leyva-Valencia I, Hernández-Guerrero CJ, Hernández-Sandoval FE, Bustillos-Guzmán JJ. 2022. Changes in toxin production, morphology and viability of *Gymnodinium catenatum* associated to allelopathy of *Chattonella marina* var. *marina* and *Gymnodinium impudicum*. Toxins. 14:616. https://doi.org/10.3390/toxins14090616

Fernández-Herrera LJ, Band-Schmidt CJ, Zenteno-Savín T, Leyva-Valencia I, Hernández-Guerrero CJ, Muñoz-Ochoa M. 2021. Cell death and metabolic stress in *Gymnodinium catenatum* induced by allelopathy. Toxins. 13:506. https://doi.org/10.3390/toxins13070506

Figueroa RI, Bravo I, Ramilo I, Pazos Y, Moroño A. 2008. New life-cycle stages of *Gymnodinium catenatum* (Dinophyceae): laboratory and field observations. Aquat Microb Ecol. 52:13-23. https://doi.org/10.3354/ame01206

Figueroa RI, Garcés E, Ramilo I. 2006. Nuclear features and effect of nutrients on *Gymnodinium catenatum* (Dinophyceae) sexual stages. J Phycol. 42:67-77. https://doi.org/10.1111/j.1529-8817.2006.00181.x

Fraga S, Gallagher SM, Anderson DM. 1989. Chain-forming dinoflagellates: an adaptation to red tides. In: Okaichi T, Anderson DM, Nemoto T (eds.), Red Tides: Biology, Environmental Science and Toxicology. New York (NY): Elsevier. p. 281-284

Gárate-Lizárraga I, Bustillos-Guzmán JJ, López-Cortés DJ, Hernández-Sandoval F, Erler K, Luckas B. 2006. Paralytic shellfish toxin profiles in net phytoplankton samples from Bahía Concepción, Gulf of California, Mexico. Mar Poll Bull. 52:800-815. https://doi.org/10.1016/j.marpolbul.2006.03.003

Green DH, Hart MC, Blackburn SI, Bolch CJS. 2010. Bacterial diversity of *Gymnodinium catenatum* and its relationship to dinoflagellate toxicity. Aquat Microb Ecol. 61:73-87. https://doi.org/10.3354/ame01437

Green DH, Llewellyn LE, Negri AP, Blackburn SI, Bolch CJ. 2004. Phylogenetic and functional diversity of the cultivable bacterial community associated with the paralytic shellfish poisoning dinoflagellate *Gymnodinium catenatum*. FEMS Microb Ecol. 47:345-357. https://doi.org/10.1016/S0168-6496(03)00298-8

Grossart HP, Simon M. 2007. Interactions of planktonic algae and bacteria: effects on algal growth and organic matter dynamics. Aquat Microb Ecol. 47:163-176.

Guillard RRL. 1973. Division rates. In: Stein JT (ed.), Handbook of phycological methods. Cambridge (UK): Cambridge University Press. p. 289-312.

Hallegraeff GM. 1993. Review of harmful algal blooms and their apparent global increase. Phycology. 32:79-99. https://doi.org/10.2216/i0031-8884-32-2-79.1

Hallegraeff GM, Blackburn SI, Doblin MA, Bolch CJS. 2011. Global toxicology, ecophysiology and population relationships of the chain forming PST dinoflagellate *Gymnodinium catenatum*. Harmful Algae. 14:130-143. https://doi.org/10.1016/j.hal.2011.10.018

Hallegraeff GM, Nichols P, Volkman JK, Blackburn SI, Everitt DA. 1991. Pigments, fatty acids and sterols of the toxic dinoflagellate *Gymnodinium catenatum*. J Phycol. 27(5):591-599. https://doi.org/10.1111/j.0022-3646.1991.00591.x

Hernández-Sandoval F, Bustillos-Guzmán JJ, Band-Schmidt CJ, Núñez-Vázquez EJ, López-Cortés DJ, Fernández-Herrera LJ, Poot-Delgado CA, Moreno-Legorreta M. 2022. Effects of different N:P ratios on the growth, toxicity, and toxin profile of *Gymnodinium catenatum* (Dinophyceae) strains from the Gulf of California. Toxins. 14:501. https://doi.org/10.3390/toxins14070501

Hernández-Sandoval FE, López-Cortés DJ, Band-Schmidt CJ, Gárate-Lizárraga I, Núñez-Vázquez EJ, Bustillos-Guzmán JJ. 2009. Toxinas paralizantes en moluscos bivalvos durante una proliferación de *Gymnodinium catenatum* Graham en la Bahía de La Paz, México. Hidrobiológica. 19:245-256.

Hold GL, Smith EA, Birkbeck TH, Gallacher S. 2001. Comparison of paralytic shellfish toxin (PST) production by the dinoflagellates *Alexandrium lusitanicum* NEPCC 253 and *Alexandrium tamarense* NEPCC 407 in the presence and absence of bacteria. FEMS Microbiol Ecol. 36:223-234. https://doi.org/10.1111/j.1574-6941.2001.tb00843.x

Hummert C, Ritscher M, Reinhardt K, Luckas B. 1997. Analysis of the characteristic PSP profiles of *Pyrodinium bahamense* and several strains of *Alexandrium* by HPLC based on ion-pair chromatographic separation, post-column oxidation, and fluorescence detection. Chromatographia. 45:312-316. https://doi.org/10.1007/BF02505576

Jauzein C, Evans AN, Erdner DL. 2015. The impact of associated bacteria on morphology and physiology of the dinoflagellate *Alexandrium tamarense*. Harmful Algae. 50:65-75.

Kepner RL, Pratt JR. 1994. Use of fluorochromes for direct enumeration of total bacteria in environmental samples: past and present. Aquat Microb Ecol. 54:603-615. https://doi.org/10.1128/mr.58.4.603-615.1994

Kirchman D, Sigda J, Kapuscinski R, Mitchell R. 1982. Statistical analysis of the direct count method for enumerating bacteria. Appl Env Microb. 44:376-382.

Lin Z-R, Geng H-X, Zhang Q-C, Chen Z-F, Dai L, Yu R-C. 2022. Toxin production of dinoflagellate *Gymnodinium catenatum* isolated from the East China Sea. Harmful Algae. 113:102188. https://doi.org/10.1016/j.hal.2022.102188

MacKenzie LA. 2014. The risk to New Zealand shellfish aquaculture from paralytic shellfish poisoning (PSP) toxins. N Z J Mar Freshw Res. 48:430-465. https://doi.org/10.1080/00288330.2014.911191

Matsumoto M. 2011. Aspects of the interaction between the marine bacterium *Alcanivorax* DG881 and the toxic dinoflagellate *Gymnodinium catenatum* [dissertation]. [Australia]: University of Tasmania. 96 p.

Mayali X, Azam F. 2004. Algicidal bacteria in the sea and their impact on algal blooms. J Eukaryot Microbiol. 51:139-144.

Medina-Elizalde J, García-Mendoza E, Turner AD, Sánchez-Bravo YA, Murillo-Martínez R. 2018. Transformation and depuration of paralytic shellfish toxins in the geoduck clam *Panopea globosa* from the Northern Gulf of California. Front Mar Sci. 5:335. https://doi.org/10.3389/fmars.2018.00335

Montoura RFC, Repeta D. 1997. Calibration methods for HPLC. In: SW Jeffrey, Mantoura RFC, Wright SW (eds.), Phytoplankton pigments in oceanography: guidelines to modern methods. Paris (France): UNESCO. p. 407-428.

Moran MA, Miller WL. 2007. Resourceful heterotrophs make the most of light in the coastal ocean. Nat Rev Microbiol. 5:792-800. https://doi:10.1038/nrmi-cro1746.

Negri AP, Bolch CJS, Geier S, Green DH, Park T-G, Blackburn SI. 2007. Widespread presence of hydrophobic paralytic shellfish toxins in *Gymnodinium catenatum*. Harmful Algae. 6:774-780.

Noman MA, Sun J, Gang Q, Guo C, Islam MS, Li S, Yue J. 2019. Factors regulating the phytoplankton and tintinnid microzooplankton communities in the East China Sea. Cont Shelf Res. 181:14-24. https://doi.org/10.1016/j.csr.2019.05.007

Palomares-García R, Bustillos-Guzmán J, Band-Schmidt CJ, López-Cortés D, Luckas B. 2006. Efecto del dinoflagelado tóxico *Gymnodinium catenatum* sobre el consumo, la producción de huevos y la tasa de eclosión del copépodo Acartia clausi. Cienc Mar. 32:111-119.

Paul C, Pohnert G. 2011. Interactions of the algicidal bacterium *Kordia algicida* with diatoms: regulated protease excretion for specific algal lysis. PLoS ONE. 6:e21032. https://doi:10.1371/journal.pone.0021032

Rippka R, Waterbury JB, Stanier RY. 1981. Isolation and purification of cyanobacteria: some general principles. In: Starr P, Stol P, Triipper H, Balows A, Sahegel H (eds.), The prokaryotes a handbook on habitats, isolation and identification of bacteria. p. 212-220.

Rooney-Varga JN, Giewat MW, Savin MC, Sood S, LeGresley M, Martin JL. 2005. Links between phytoplankton and bacterial community dynamics in a coastal marine environment. FEMS Microb Ecol. 49:75-163. https://doi.org/10.1007/s00248-003-1057-0

Seibold A, Wichels A, Schütt C. 2001. Diversity of endocytic bacteria in the dinoflagellate *Noctiluca scintillans*. Aquat Microb Ecol. 25:229-235.

Sherr EB, Caron DA, Sherr BF. 1993. Staining of heterotrophic protists for visualization via epifluorescence microscopy. In: Kemp P, Sherr B, Sherr E, Cole J (eds.), Current Methods in Aquatic Microbial Ecology. New York (NY): Lewis Publishing Company. p. 213-228

Skovgaard A. 2000. A phagotrophically derivable growth factor in the plastidic dinoflagellate *Gyrodinium resplendens* (Dinophyceae). J Phycol. 36:1096-1078.

Throndsen J. 1979. Special methods-micromanipulators. In: Stein RJ (ed.), Handbook of Phycological Methods: Culture Methods and Growth Measurements. Cambridge (UK): Cambridge University Press. p. 139-144.

Vale P. 2015. Effects of light and salinity stresses in production of mycosporine-like amino acids by *Gymnodinium catenatum* (Dinophyceae). Photochem Photobiol. 91:1112-1122.

Vale P. 2017. Influence of static magnetic fields in phototaxis and osmotic stress in *Gymnodinium catenatum* (Dinophyceae). Gen Physiol Biophys. 36:235-245.

Vidussi F, Claustre H, Bustillos-Guzmán JJ, Cailleau C, Marty JC. 1996. Rapid HPLC method for determination of phytoplankton chemotaxonomic pigments: separation of chlorophyll *a* from divinyl-chlorophyll *a* and zeaxanthin from lutein. J Plank Res. 18:2377-2382.

Vives CR, Schallenberg C, Strutton PG, Westwood KJ. 2022. Iron and light limitation of phytoplankton growth off East Antarctica. J Mar Syst. 234:103774. https://doi.org/10.1016/j.jmarsys.2022.103774

Wang H, Tomasch J, Jarek M, Wagner-Döbler I. 2014. A dual-species co-cultivation system to study the interactions between *Roseobacters* and dinoflagellates. Front Microbiol. 5:00311. https://doi.org/10.3389/fmicb.2014.00311

Yu RC, Hummert C, Luckas B, Qian PY, Zhou MJ. 1998. Modified HPLC method for analysis of PSP toxins in algae and shellfish from China. Chromatographia. 48:671-676. https://doi.org/10.1007/BF02467597

Zar JH. 1999. Biostatistical analysis (4th ed.). Saddle River (USA): Prentice-Hal. 1046 p.

Zheng L, Lin H, Balaji-Prasath B, Su Y, Wang Y, Zheng Y, Yu G. 2023. A novel algicidal properties of fermentation products from *Pseudomonas* sp. Ps3 strain on the toxic red tide dinoflagellate species. *Front Microbiol*. 14:1146325. https://doi.org/10.3389/fmicb.2023.1146325